

StyleDiffusion: Prompt-Embedding Inversion for Text-Based Editing

Senmao Li¹, Joost van de Weijer², Taihang Hu¹, Fahad Shahbaz Khan³, Qibin Hou¹,
 Yaxing Wang¹(✉), Jian Yang¹, Ming-Ming Cheng¹

© The Author(s) 2015.

Abstract A significant research effort is focused on exploiting the amazing capacities of pretrained diffusion models for the editing of images. They either finetune the model, or invert the image in the latent space of the pretrained model. However, they suffer from two problems: (1) Unsatisfying results for selected regions and unexpected changes in non-selected regions. (2) They require careful text prompt editing where the prompt should include all visual objects in the input image. To address this, we propose two improvements: (1) Only optimizing the input of the value linear network in the cross-attention layers is sufficiently powerful to reconstruct a real image. (2) We propose attention regularization to preserve the object-like attention maps after reconstruction and editing, enabling us to obtain accurate style editing without invoking significant structural changes. We further improve the editing technique that is used for the unconditional branch of classifier-free guidance as used by P2P. Extensive experimental prompt-editing results on a variety of images demonstrate qualitatively and quantitatively that our method has superior editing capabilities compared to existing and concurrent works. See our accompanying code in StyleDiffusion: <https://github.com/sen-mao/StyleDiffusion>.

Keywords Real-image inversion, Image editing, Diffusion models.

¹ College of Computer Science, Nankai University, Tianjin, China 300350.

² The Computer Vision Center, Universitat Autònoma de Barcelona, Barcelona 08193, Spain. E-mail: joost@cvc.uab.es.

³ Mohamed bin Zayed University of Artificial Intelligence (UAE), and Linkoping University (Sweden). E-mail: fahad.khan@liu.se.

Manuscript received: 2024-06-12; accepted: 2024-09-30

1 Introduction

Text-based deep generative models have achieved extensive adoption in the field of image synthesis. Notably, GANs [20, 31, 50, 59], diffusion models [17, 53, 56, 58], autoregressive models [74], and their hybrid counterparts have been prominently utilized in this domain.

Diffusion models have made remarkable progress due to their exceptional realism and diversity. It has seen rapid applications in other domains such as video generation [33, 69, 79], 3D generation [41, 51, 67] and speech synthesis [27, 29, 36]. In this work, we focus on Stable Diffusion (SD) models for real image editing. This capability is important for many real-world applications, including object replacement in images for publicity purposes (as well as personalized publicity), dataset enrichment where rare objects are added to datasets (e.g. wheelchairs in autonomous driving datasets), furniture replacement for interior design, etc.

Researchers basically perform real image editing with two steps: *projection* and *manipulation*. The former aims to either adapt the weights of the model [34, 43, 60, 71] or project given images into the latent code or embedding space of SD models [5, 18, 22, 46]. The latter aims to edit the latent code or embedding to further manipulate real images [10, 13, 32, 44, 75]. In the first *projection* step, some works finetune the whole model [19, 32, 34, 57, 65, 71] or partial weights of the pretrained model [37, 72]. Yet, finetuning either the entire or part of the generative model with only a few real images suffers from both the cumbersome tuning of the model's weights and catastrophic forgetting [37, 68, 72]. Other works on *projection* attempt to learn a new embedding vector which represents given real images (keeping the SD model frozen) [5, 16, 18, 22, 26, 61, 77]. They focus on optimizing conditional or unconditional

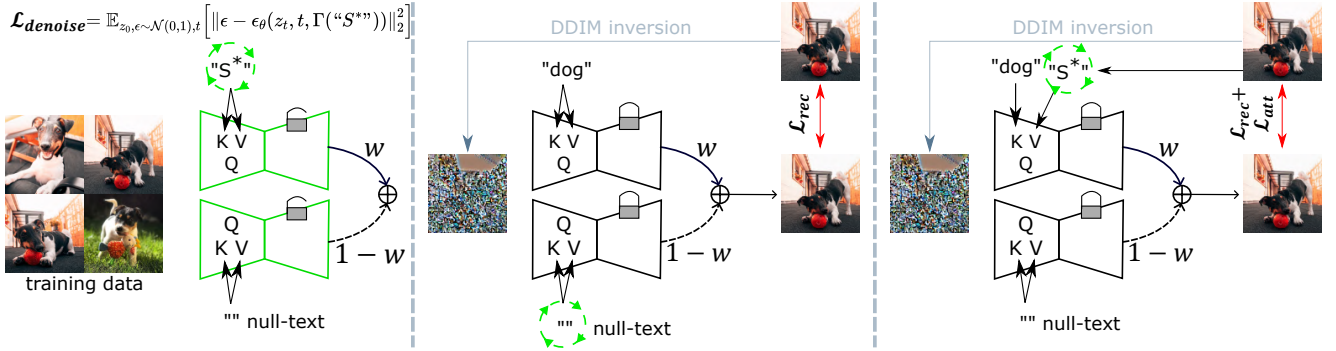


Figure 1 Three different optimization methods for inverting real image(s). (Left) Some works invert the image(s) into a new textual embedding “ S^* ” by finetuning the pretrained diffusion model or freezing the model and applying a denoising loss $\mathcal{L}_{denoise}$. Here, w is the classifier-free guidance parameter. These methods require a few training images. (Middle) Null-text inversion optimizes the null-text embedding with the reconstruction loss. (Right) Our Stylediffusion maps the real image to the input embedding of the *value* of the cross-attention, enabling accurate style editing without causing significant structural changes.

inputs of the cross-attention layers of the classifier-free diffusion model [26]. Textual Inversion [18] uses the denoising loss to optimize the textual embedding of the conditional branch given a few content-similar images. Null-text optimization [46] firstly inverts the real image into a series of timestep-related latent codes, then leverages a reconstruction loss to learn the null-text embedding of the unconditional branch (see Fig. 1(middle)). However, these methods suffer from the following issues. **Firstly**, they lead to unsatisfactory results for selected regions, and unexpected changes in non-selected regions, both during reconstruction and editing (see the Null-text results in Fig. 2; the structure-dist (\downarrow) for Null-text Editing and editing by our method are 0.046 and 0.012 in the first row, and 0.019 and 0.054 in the second row). **Secondly**, they require a user to provide an accurate text prompt that describes every visual object, and the relationships between them in the input image (see Fig. 3). **Finally**, Pix2pix-zero [49] requires the textual embedding directions (e.g, cat \rightarrow dog in Fig. 9(up, the fourth column)) with thousands of sentences with GPT-3 [9] before editing, which lacks scalability and flexibility.

To overcome the above-mentioned challenges, we analyze the role of the attention mechanism (and specifically the roles of keys, queries and values) in the diffusion process. This leads to the observation that the key dominates the output image structure (the “where”) [24], whereas the value determines the object style (the “what”). We perform an effective experiment to demonstrate that the value determines the object style (the “what”). As shown in Fig. 4(top), we generate two sets of images with prompt embeddings \mathbf{c}_1 and \mathbf{c}_2 . We use two different embeddings for the

input of both key and value in the same attention layer. When swapping the input of the keys and fixing the input of the values, we observe that the content of generated images are similar, see Fig. 4(middle). For example, The images of Fig. 4(middle) are similar to the ones of Fig. 4(top). When exchanging the input of the values and fixing the one of the keys, we find that the content swaps while preserving much of the structure, see Fig. 4(bottom). For example, the images of the last row of Fig. 4(bottom) have similar semantic information with the ones of the first row of Fig. 4(top). It should be noted that their latent codes are all shared¹, so the structure of the results in Fig. 4(middle) does not change significantly. This experiment indicates that the value determines the object’s style (the “what”).

Therefore, to improve the projection of a real image, we introduce **Stylediffusion** which maps a real image to the input embedding for the value computation (we refer to this embedding as the **prompt-embedding**), which enables us to obtain accurate style editing without invoking significant structural changes. We propose to map the real image to the input of the *value* linear layer in the cross-attention layers [8, 66] providing freedom to edit effectively the real image in the manipulation step.

We take the given textual embedding as the input of the *key* linear layer, which is frozen (see Fig. 1(right)). Using frozen embedding contributes to preserving the well-learned attention map from DDIM inversion, which guarantees the initial editability of the inverted image. We observe that the system often outputs unsatisfactory reconstruction results (greatly adjusting

¹The first row of top, middle, and bottom shares a common latent code, and the second row also shares a common latent code.

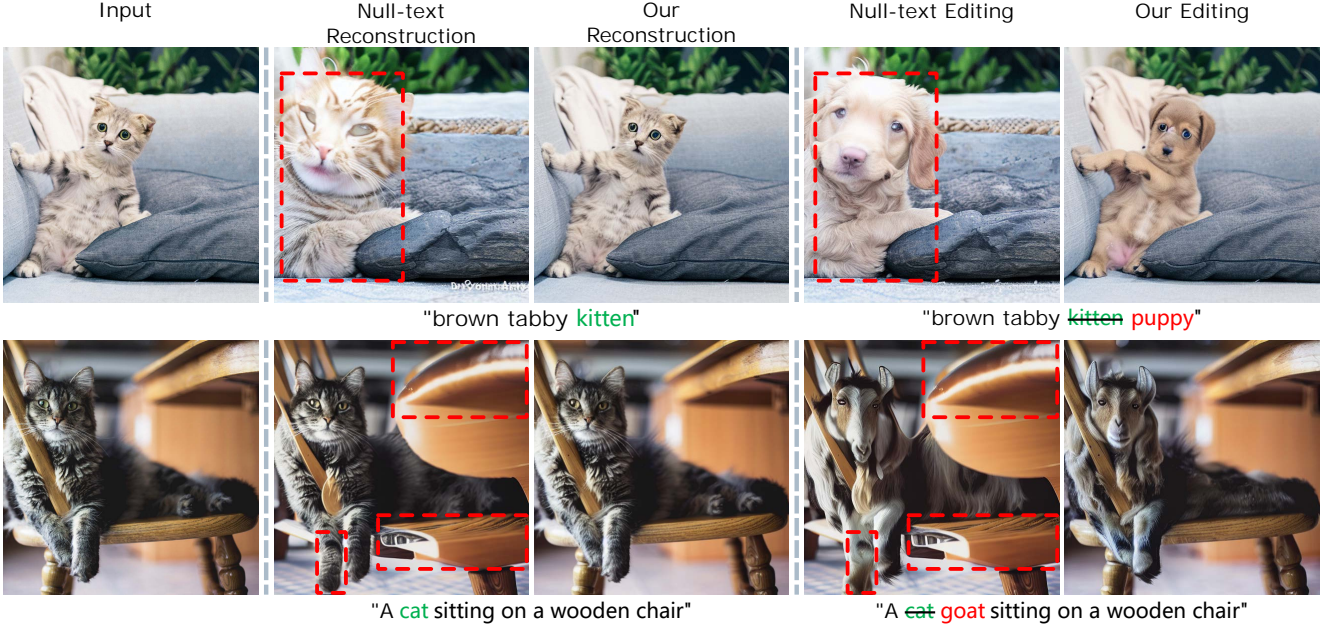


Figure 2 Our method takes as an input a real image (leftmost column) and an associated caption. Here we demonstrate more accurate reconstruction and editing capabilities compared to Null-text. We manipulate the inverted image using the P2P editing technique.

the input image structure) (see Fig. 2(first row, second column) and Fig. 15(first row, second column)) due to locally less accurate attention maps (see Fig. 15(first row, and third column)). Hence, to further improve our method, we propose an attention regularization to obtain more precise reconstruction and editing capabilities.

For the second manipulation step, researchers propose a series of outstanding techniques [10, 13, 30, 32, 40, 44, 47, 52, 75, 78]. Among them, P2P [24] is one of the most widely used image editing methods. However, P2P only operates on the conditional branch, and ignores the unconditional branch. This leads to less accurate editing capabilities for some cases, especially where the structural changes before and after editing are relatively large (e.g., “...tree...” → “...house...” in Fig. 5). To address this problem, we need to reduce the dependence of the structure on the source prompt and provide more freedom to generate the structure following the target prompt. Since the unconditional branch allows us to edit out concepts [4, 64]. Thus, we propose to further perform the self-attention map exchange in the unconditional branch based on P2P (referred to as *P2Plus*), as well as in the conditional branch like P2P [24]. This technique enables us to obtain more accurate editing capabilities (see Fig. 5(third column)). We build our method on SD models [56] and experiment on a variety of images and several ways of prompt editing.

Our work thus makes the following contributions:

- State-of-the-art methods (e.g., Null-text inversion) struggle with unsatisfactory reconstruction and editing. To precisely project a real image, we introduce **StyleDiffusion**. We use a simple mapping network to map a real image to the input embedding for *value* computation.
- We propose an attention regularization method to enhance the precision of attention maps, resulting in more accurate reconstructions and improved editing capabilities.
- We propose the P2Plus technique, which enables us to obtain more powerful editing capabilities, especially when the source object is unrelated to the target object. This approach addresses the limitations of P2P, which fails to function effectively in such cases.
- Through extensive experiments, we demonstrate the effectiveness of our method for accurately reconstructing and editing images.

2 Related work

2.1 Transfer learning for diffusion models

A series of recent works has investigated knowledge transfer on diffusion models [5, 16, 18, 19, 22, 34, 38, 39, 43, 46, 60, 61, 71, 77] with one or a few images. Recent work [10, 11, 13, 30, 32, 40, 44, 47, 52, 75, 78] either finetune the pretrained model or invert the image in the

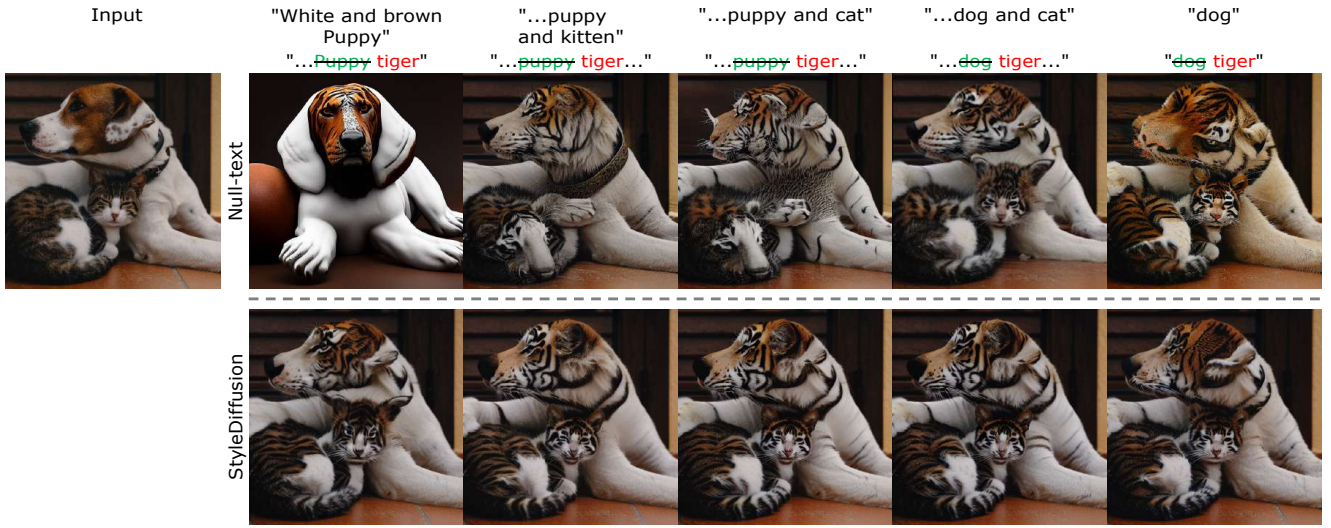


Figure 3 Null-text editing results of a real image with different prompts. A satisfactory result requires a carefully selected prompt.

latent space of the pretrained model. Dreambooth [57] shows that training a diffusion model on a small data set (of $3 \sim 5$ images) largely benefits from a pretrained diffusion model, preserving the textual editing capability. Similarly, Imagic [32] and UniTune [65] rely on the interpolation weights or the classifier-free guidance at the inference stage, except when finetuning the diffusion model during training. Kumari et al. [37] study only updating part of the parameters of the pretrained model, namely the *key* and *value* mapping from text to latent features in the cross-attention layers. However, updating the diffusion model unavoidably loses the text editing capability of the pre-trained diffusion model. In this paper, we focus on real image editing with a frozen text-guilded diffusion model.

2.2 GAN inversion

Image inversion aims to project a given real image into the latent space, allowing users to further manipulate the image. There exist several approaches [14, 21, 28, 42, 70, 73] which focus on image manipulation based on pre-trained GANs, following literately optimization of the latent representation to restructure the target image. Given a target semantic attribute, they aim to manipulate the output image of a pretrained GAN. Several other methods [1, 80] reverse a given image into the input latent space of a pretrained GAN (e.g., StyleGAN), and restructure the target image by optimization of the latent representation. They mainly consist of fixing the generator [1, 2, 54, 62] or updating the generator [3, 55].

2.3 Diffusion model inversion

Diffusion-based inversion can be performed naively by optimizing the latent representation. [15] show that a given real image can be reconstructed by DDIM sampling [60]. DDIM provides a good starting point to synthesize a given real image. Several works [6, 7, 48] assume that the user provides a mask to restrict the region in which the changes are applied, achieving both meaningful editing and background preservation. P2P [24] proposes a mask-free editing method. However, it leads to unexpected results when editing the real image [46]. Recent work investigates the text embedding of the conditional input [18], or the null-text optimization of the unconditional input (i.e., Null-text inversion [46]). Although having the editing capability by combining the new prompts, they suffer from the following challenges (i) they lead to unsatisfying results for the selected regions, and unexpected changes in non-selected regions, and (ii) they require careful text prompt editing where the prompt should include all visual objects in the input image.

Concurrent work [49] proposes pix2pix-zero, also aiming to provide more accurate editing capabilities of the real image. However, it firstly needs to compute the textual embedding direction in advance using thousand sentences.

3 Method

3.1 Background

DDIM inversion proposes an inversion scheme for unconditional diffusion models. However, this method

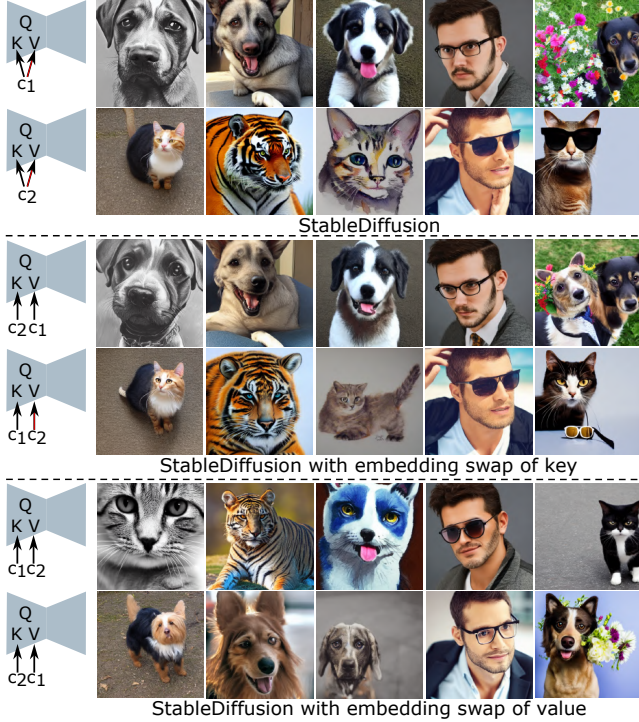


Figure 4 (Top) from second to last columns, the prompts corresponding to both \mathbf{c}_1 and \mathbf{c}_2 are [“Dog”, “Dog”, “Dog”, “A man in glasses”, “A dog holding flowers”] and [“Cat”, “Tiger”, “Watercolor drawing of a cat”, “A man in sunglasses”, “A cat wearing sunglasses”], in turn. (Middle) we swap the input embedding of the *key* and fix the one of the *value*. This result shows that the generated images in both the third and fourth rows are similar to the ones in both the first and second rows, respectively. (Bottom) we fix the input embedding of the *key* and swap the one of the *value*. This experiment indicates that the *value* determines the object style (the “what”).

fails when applied to text-guided diffusion models. This was observed by Mokady et al. [46], who propose Null-text inversion to address this problem. However, their methods has some drawbacks: (1) unsatisfying results for selected regions and unexpected changes in non-selected regions, and (2) they require careful text prompt editing where the prompt should include all visual objects in the input image.

Therefore, our goal is to obtain a more accurate editing capability based on an accurate reconstruction of the real image \mathbf{x} guided by the source prompt \mathbf{p}^{src} . Our method, called StyleDiffusion, is based on the observation that the *keys* of the cross-attention layer dominate the output image structure (the “where”), whereas the *values* determine the object style (the “what”). After faithfully projecting the real image, we propose P2Plus, which is an improved version of P2P [24].

Next, we introduce SD models in Sec. 3.2, followed

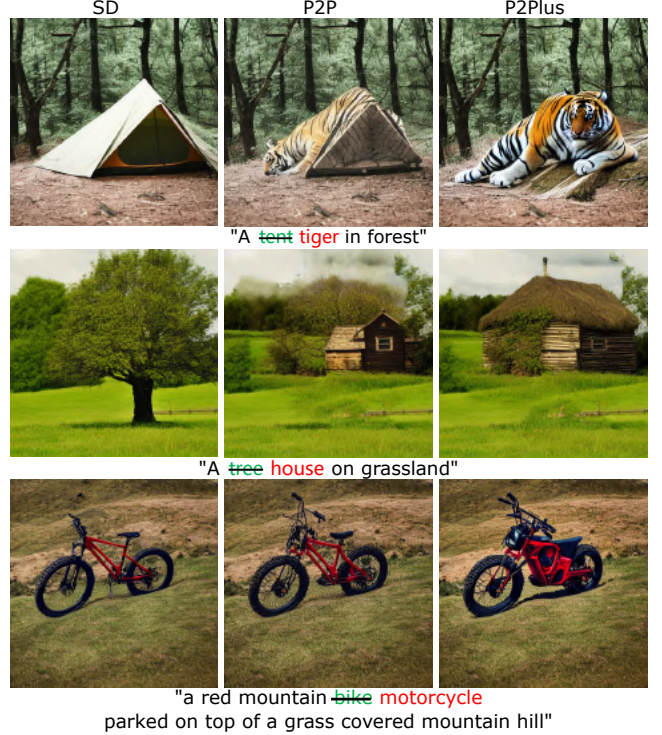


Figure 5 Comparison of both P2P and P2Plus. P2P fails when the desired editing changes require large structural changes (e.g., tent, tree, and bike). By reducing the dependence on the source prompt (by also involving the unconditional branch), P2Plus can better handle such cases. The Clipscore (\uparrow) of P2P and P2Plus are 84.2% and 87.2% in the first row, 77.6% and 78.4% in the second row, and 70.8% and 78.6% in the third row.

by the proposed StyleDiffusion in Sec. 3.3 and P2Plus in Sec. 3.4. A general overview is provided in Fig. 6.

3.2 Preliminary: Diffusion Model

3.2.1 Basis

Generally, diffusion models optimize a UNet-based denoiser network ϵ_θ to predict Gaussian noise ϵ , following the objective:

$$\min_{\theta} E_{\mathbf{z}_0, \epsilon \sim N(0, I), t \sim [1, T]} \|\epsilon - \epsilon_\theta(\mathbf{z}_t, t, \mathbf{c})\|_2^2, \quad (1)$$

where z_t is a noise sample according to timestep $t \sim [1, T]$, and T is the number of the timesteps. The encoded text embedding \mathbf{c} is extracted by a Clip-text Encoder Γ with given prompt \mathbf{p}^{src} : $\mathbf{c} = \Gamma(\mathbf{p}^{src})$. In this paper, we build on SD models [56]. These first train both encoder and decoder. Then the diffusion process is performed in the latent space. Here the encoder maps the image \mathbf{x} into the latent representation \mathbf{z}_0 , and the decoder aims to reverse the latent representation \mathbf{z}_0

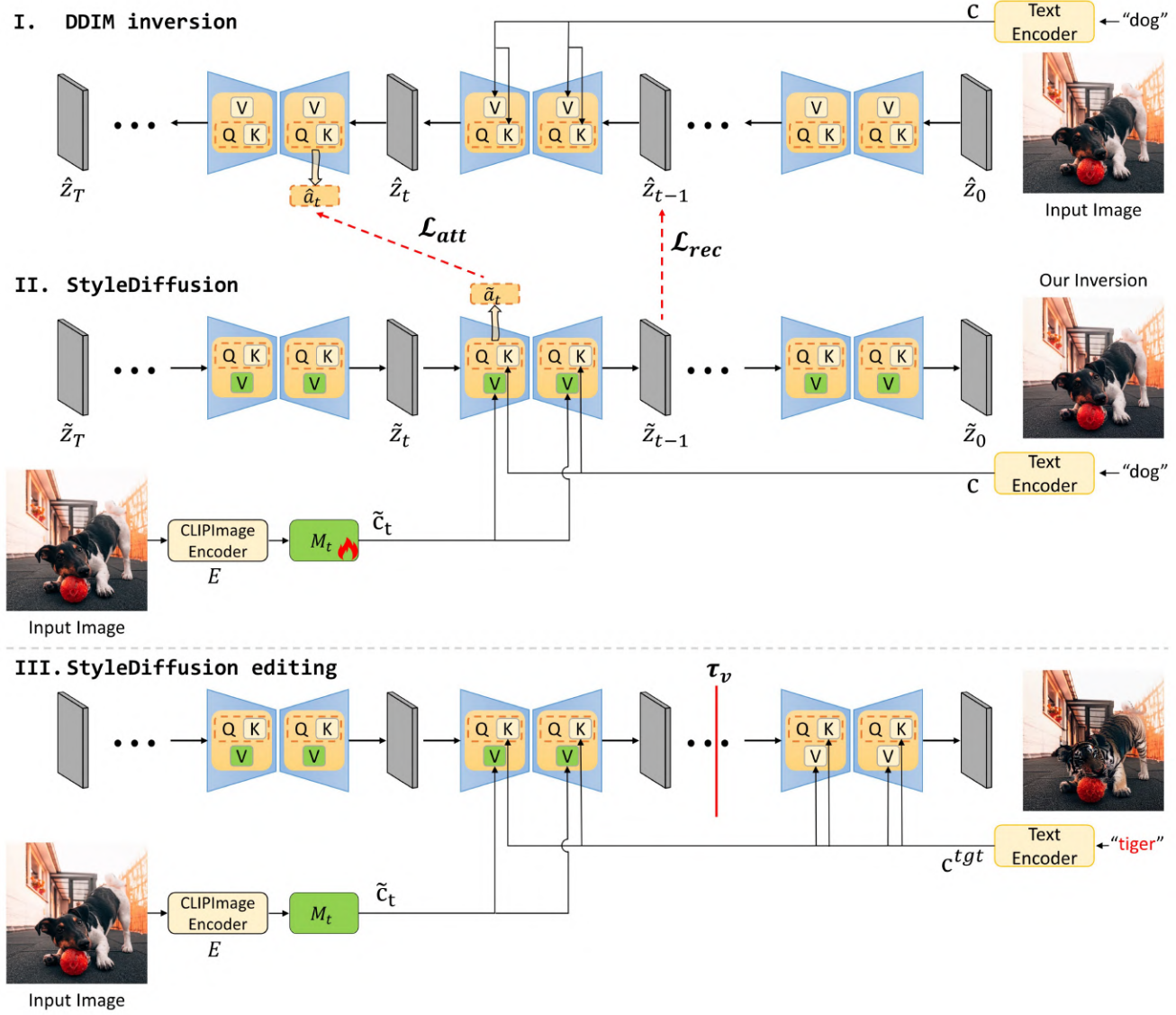


Figure 6 Overview of the proposed method. (I) DDIM inversion: the diffusion process is performed to generate the latent representations: $(\hat{\mathbf{z}}_t, \hat{\mathbf{a}}_t), (t = 1, \dots, T)$, where $\hat{\mathbf{z}}_0 = \mathbf{z}_0$, which is the extracted feature of the input real image \mathbf{x} . \mathbf{c} is the textual embedding extracted by a Clip-text Encoder with a given prompt \mathbf{p}^{src} . (II) StyleDiffusion: we take the input image \mathbf{x} as input, and extract the prompt-embedding $\tilde{\mathbf{c}}_t = M_t(E(\mathbf{x}))$, which is taken as the input value matrix \mathbf{v} of the linear layer Ψ_V . The input of the linear layer Ψ_K is the given textual embedding \mathbf{c} . We get both the latent code $\hat{\mathbf{z}}_{t-1}$ and the attention map $\hat{\mathbf{a}}_t$, which are aligned with both the latent code $\hat{\mathbf{z}}_T$ and the attention map $\hat{\mathbf{a}}_T$, respectively. Note that $\hat{\mathbf{z}}_T = \hat{\mathbf{z}}_T$. (III) StyleDiffusion editing: for timesteps from T to τ_v , the input of the linear network Ψ_v comes from the learned textual embedding $\tilde{\mathbf{c}}_t$ produced by the trained M_t . From $\tau_v - 1$ to 1 the corresponding input comes from the prompt-embedding \mathbf{c}^{tgt} of the target prompt. We use P2Plus to perform the attention exchange.

into the image. The sampling process is given by:

$$\mathbf{z}_{t-1} = \sqrt{\frac{\alpha_{t-1}}{\alpha_t}} \mathbf{z}_t + \sqrt{\alpha_{t-1}} \left(\sqrt{\frac{1}{\alpha_{t-1}} - 1} - \sqrt{\frac{1}{\alpha_t} - 1} \right) \epsilon_\theta(\mathbf{z}_t, t, \mathbf{c}), \quad (2)$$

where α_t is a scalar function.

3.2.2 DDIM inversion

For real-image editing with a pretrained diffusion model, a given real image is to be reconstructed by finding its initial noise. We use the deterministic DDIM model to perform image inversion. This process is given

by:

$$\mathbf{z}_{t+1} = \sqrt{\frac{\alpha_{t+1}}{\alpha_t}} \mathbf{z}_t + \sqrt{\alpha_{t+1}} \left(\sqrt{\frac{1}{\alpha_{t+1}}} - 1 - \sqrt{\frac{1}{\alpha_t}} - 1 \right) \epsilon_\theta(\mathbf{z}_t, t, \mathbf{c}). \quad (3)$$

DDIM inversion synthesizes the latent noise that produces an approximation of the input image when fed to the diffusion process. While the reconstruction based on DDIM is not sufficiently accurate, it still provides a good starting point for training, enabling us to efficiently achieve high-fidelity inversion [24]. We use the intermediate results of DDIM inversion to train our model, similarly as [13, 46].

3.2.3 Cross-attention

SD models achieve text-driven image generation by feeding a prompt into the cross-attention layer. Given both the text embedding \mathbf{c} and the image feature representation \mathbf{f} , we are able to produce the key matrix $\mathbf{k} = \Psi_K(\mathbf{c})$, the value matrix $\mathbf{v} = \Psi_V(\mathbf{c})$ and the query matrix $\mathbf{q} = \Psi_Q(\mathbf{f})$, via the linear networks: Ψ_K, Ψ_V, Ψ_Q . The attention maps are then computed with:

$$\mathbf{a} = \text{Softmax}(\mathbf{q}\mathbf{k}^T / \sqrt{d}), \quad (4)$$

where d is the projection dimension of the keys and queries. Finally, the cross-attention output is $\hat{\mathbf{f}} = \mathbf{a}\mathbf{v}$, which is then taken as input in the following convolution layers.

Intuitively, P2P [24] performs prompt-to-prompt image editing with cross attention control. P2P is based on the idea that the attention maps largely control where the image is drawn, and the values decide what is drawn (mainly defining the style). Improving the accuracy of the attention maps leads to more powerful editing capabilities [46]. We experimentally observe that DDIM inversion generates satisfying attention maps (e.g., Fig. 15(second row, first column)), and provides a good starting point for the optimization. Next, we investigate the attention maps to guide the image inversion.

3.3 StyleDiffusion

3.3.1 Method overview

As shown in Fig. 6(I), given a pair of a real image \mathbf{x} and a corresponding prompt \mathbf{p}^{src} (e.g., "dog"), we perform DDIM inversion [15, 60] to synthesize a series of latent noises $\{\hat{\mathbf{z}}_t\}$ and attention maps $\{\hat{\mathbf{a}}_t\}$ ($t = 1, \dots, T$), where $\hat{\mathbf{z}}_0 = \mathbf{z}_0$, which is the extracted latent code of the input image \mathbf{x} ². Fig. 6(II) shows that our

²Note when generating the attention map $\hat{\mathbf{a}}_T$ in the last timestep $t = T$, we throw out the synthesized latent code $\hat{\mathbf{z}}_{T+1}$.

Algorithm 1: Our algorithm

Require: the features of the training image and the prompt embeddings: $\{\mathbf{z}_0, \mathbf{c}\}$. $K_t = e^{-t} * K$, where $K = 100$, the starting number of inner iterations. K_t is the number of training iteration for each timestep t . The mapping network $\{M_t\}$, ($t = 1, \dots, T$) with initialization parameters ω .
Temporary results: With guidance scale $w = 1$ for the classifier-free diffusion model, we use DDIM inversion to produce $\{\hat{\mathbf{z}}_j, \hat{\mathbf{a}}_j\}$, ($j = 1, \dots, T$).
Output: Mapping network $\{M_t\}$, ($t = 1, \dots, T$).
Set guidance scale $w = 7.5$;
Initializing $\tilde{\mathbf{z}}_T \leftarrow \hat{\mathbf{z}}_T$;
for $t = T, T-1, \dots, 1$ **do**
 for $k = 0, \dots, K_t - 1$ **do**
 $\mathbf{a}_t, \mathbf{z}_{t-1} \leftarrow \tilde{\mathbf{z}}_t$; (Eqs. 4 and 6)
 $\omega \leftarrow \omega - \eta \nabla_\omega \mathcal{L}$; (Eq. 8)
 end for
 Synthesizing $\tilde{\mathbf{z}}_{t-1}$; (Eq. 6)
end for
Return Mapping network $\{M_t\}$, ($t = 1, \dots, T$)

method reconstructs the latent noise $\hat{\mathbf{z}}_t$ in the order of the diffusion process $T \rightarrow 0$, where $\tilde{\mathbf{z}}_T = \hat{\mathbf{z}}_T$. Our framework consists of three networks: a frozen ClipImageEncoder E , a learnable mapping network M_t and a denoiser network ϵ_θ . For a specific timestep t , the ClipImageEncoder E takes the input image \mathbf{x} as an input. The output $E(\mathbf{x})$ is fed into the mapping network M_t , producing the prompt-embedding $\tilde{\mathbf{c}}_t = M_t(E(\mathbf{x}))$, which is fed into the value network Ψ_V of the cross-attention layers. The input of the linear layer Ψ_K is the given textual embedding \mathbf{c} . We generate both the latent code $\tilde{\mathbf{z}}_{t-1}$ and the attention map $\tilde{\mathbf{a}}_t$. Our full algorithm is presented in algorithm 1.

The full loss function consists of two losses: *reconstruction loss* and *attention loss*, which guarantee that both the denoised latent code $\tilde{\mathbf{z}}_{t-1}$ and the corresponding attention map $\tilde{\mathbf{a}}_t$ at inference time are close to the ones: $\hat{\mathbf{z}}_{t-1}$ and $\hat{\mathbf{a}}_t$ from DDIM inversion, respectively.

3.3.2 Reconstruction loss

Since the noise representations ($\{\hat{\mathbf{z}}_1, \dots, \hat{\mathbf{z}}_T\}$) provide an initial trajectory which is close to the real image, we train the network M_t to generate the prompt embedding $\tilde{\mathbf{c}}_t = M_t(E(\mathbf{x}))$, which is the input of the value network. We optimize the M_t in such a manner, that the output latent code ($\tilde{\mathbf{z}}_t$) is close to the noise representations ($\hat{\mathbf{z}}_t$). The objective is:

$$\mathcal{L}_{\text{rec}} = \min_{M_t} \|\hat{\mathbf{z}}_{t-1} - \tilde{\mathbf{z}}_{t-1}\|^2, \quad (5)$$

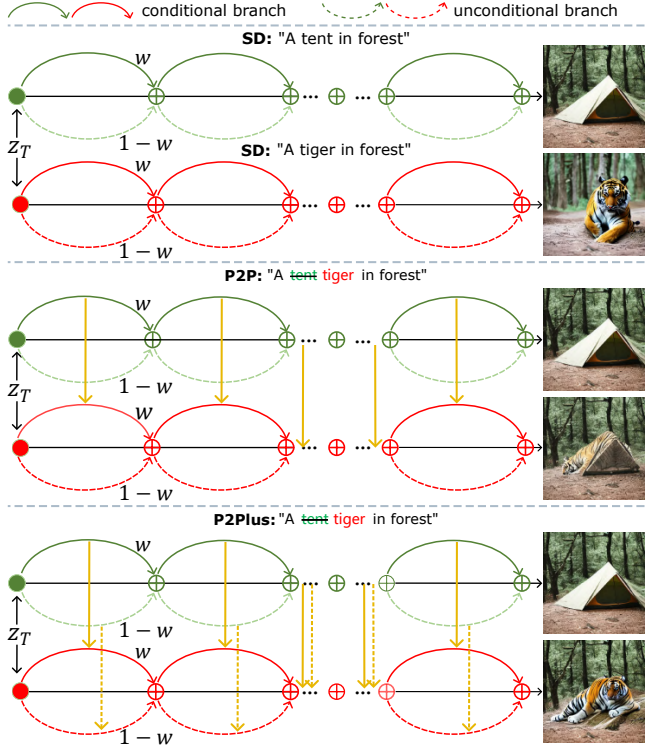


Figure 7 (Top) Given the same latent code \mathbf{z}_T and the classifier-free guidance parameter w , we generate two images with two prompts. The arrows indicate the diffusion process from T to 0. Here green indicates generation using the source prompt: “A tent in forest” and red indicates generation using the target prompt: “A tiger in forest”. (Middle) P2P copies both the self-attention maps and the cross-attention maps of the conditional branch of the SD models from the source prompt into the corresponding self-attention and cross-attention maps of the conditional branch of the SD models with target prompt. This process is indicated by yellow arrows. (Bottom) P2Plus additionally replaces the self-attention map of the unconditional branch of SD models, in addition to the ones of the conditional branch. The dashed yellow arrows indicate this technique.

$$\tilde{\mathbf{z}}_{t-1} = \sqrt{\frac{\alpha_{t-1}}{\alpha_t}} \tilde{\mathbf{z}}_t + \sqrt{\alpha_{t-1}} \left(\sqrt{\frac{1}{\alpha_{t-1}} - 1} - \sqrt{\frac{1}{\alpha_t} - 1} \right) \epsilon_{\theta}(\tilde{\mathbf{z}}_t, t, \mathbf{c}, \mathbf{c}_t). \quad (6)$$

3.3.3 Attention loss

It is known that a more accurate attention map is positively correlated to the editing capability [46]. The attention map, which is synthesized during the DDIM inversion, provides a good starting point. Thus, we introduce attention regularization when optimizing the mapping network M_t to further improve its quality. The objective is the following:

$$\mathcal{L}_{\text{att}} = \min_{M_t} \|\hat{\mathbf{a}}_t - \tilde{\mathbf{a}}_t\|^2, \quad (7)$$

where $\hat{\mathbf{a}}_t$ and $\tilde{\mathbf{a}}_t$ can be obtained with Eq. 4.

3.3.4 Full objective

The full objective function of our model is:

$$\mathcal{L} = \mathcal{L}_{\text{rec}} + \mathcal{L}_{\text{att}}. \quad (8)$$

In conclusion, in this section, we have proposed an alternative solution to the inversion of text-guided diffusion models which aims to improve upon existing solutions by providing more accurate editing capabilities, without requiring careful prompt engineering.

3.4 P2Plus

Having inverted the text-guided diffusion model, we can now perform prompt-based image editing (see Figs. 2 and 9). We here outline our approach, which improves on the popular P2P

P2P performs the replacement of both the cross-attention map and the self-attention map of the conditional branch, aiming to maintain the structure of the source prompt, see Fig. 7(middle). However, it ignores the replacement in the unconditional branch. This leads to less accurate editing in some cases, especially when the structural changes before and after editing are relatively large (e.g., “...tent...” → “...tiger...”). To address this problem, we need to reduce the dependence of the structure on the source prompt and provide more freedom to generate the structure following the target prompt. Thus, as shown in Fig. 7(bottom) we propose to further perform the self-attention map replacement in the unconditional branch based on P2P (an approach we call *P2Plus*), as well as in the conditional branch like P2P. This technique provides more accurate editing capabilities. Like P2P, we introduce a timestep parameter τ_u that determines until which step the injection is applied. Fig. 8 shows the results with different τ_u values.

4 Experimental setup

4.1 Training details and datasets

We use the pretrained Stable Diffusion model. The configuration of the mapping network M_t is provided in Tab. 1. We set $T = 30$. τ_v is a timestep parameter that determines which timestep is used by the output of the mapping network in the StyleDiffusion editing phase. Similarly, we can set the timestep τ_u (as in the conditional branch in P2P) to control the number of diffusion steps in which the injection of the unconditional branch is applied. We use Adam [35] with a batch size of 1 and a learning rate of 0.0001. The exponential decay rates are $(\beta_1, \beta_2) = (0, 0.999)$. We randomly initialize the weights of the mapping network

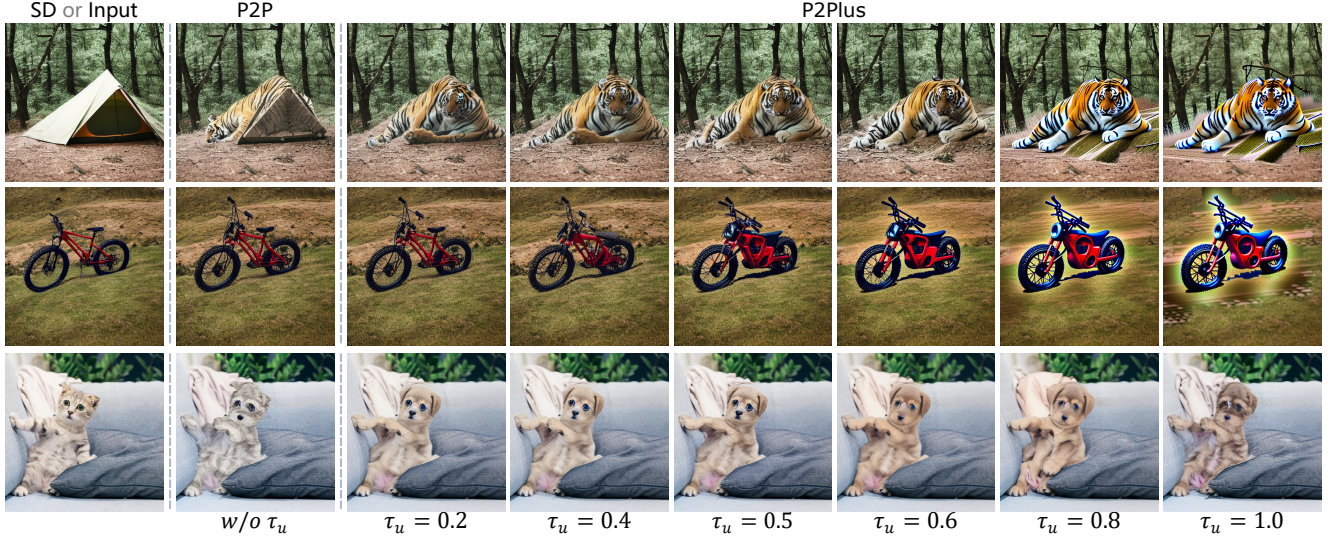


Figure 8 *P2P* (i.e., second column: w/o τ_u) has not succeeded in replacing the tent by the tiger. Adding the injection parameter τ_u can help to edit successfully, especially if $\tau_u = 0.5$. We also use the classifier-free guidance parameter $w = 7.5$ like SD, when the weight $1 - w$ of the unconditional branch is negative, which can gradually weaken the influence of the “tent” in the unconditional branch as τ_u increases from 0.2 to 1.0 (third to eighth columns). The source images in the first and second rows are from SD, while the source image in the third row is from the input real image (first column). Editing from the first to the third row are “...tent...” → “...tiger...”, “...bike...” → “...motorcycle...”, and “...kitten...” → “...puppy...”.

following a Gaussian distribution centered at 0 with 0.01 standard deviation. We use one Quadro RTX 3090 GPUs (24 GB VRAM) to conduct all our experiments. We randomly collect a real image dataset of 100 images (with resolution 512×512) and caption pairs from Unsplash(<https://unsplash.com/>) and COCO [12].

4.2 Evaluation metrics

Clipscore [25] is a metric that evaluates the quality of a pair of a prompt and an edited image. To evaluate the preservation of structure information after editing, we use Structure Dist [63] to compute the structural consistency of the edited image. Furthermore, we aim to modify the selected region, which corresponds to the target prompt, while preserve the non-selected region. Thus, we also need to evaluate change in the non-selected region after editing. To automatically determine the non-selected region of the edited image, we use a binary method to generate the raw mask from the attention map. Then we invert it to get the non-selected region mask. Using the non-selected region mask, we compute the non-selected region LPIPS [76] between the real and edited images, which we denote *NS-LPIPS* for non-selected LPIPS. A lower NS-LPIPS score means that the non-selected region is more similar to the input image. We also use both PSNR and SSIM to evaluate image reconstruction.

Table 1 Configuration of mappingnetwork M_t . C_I , C_O denote numbers of input and output channels.

Metric	(Input channel, Output channel)	(Kernal size, Stride)	Input dimension	Output dimension
Conv0	(197, 77)	(1, 1)	(197, 768)	(77, 768)
Conv1	(77, 77)	(1, 1)	(77, 768)	(77, 768)
BatN1	-	-	(77, 768)	(77, 768)
LeakyRelu1	-	-	(77, 768)	(77, 768)
Conv2	(77, 77)	(1, 1)	(77, 768)	(77, 768)

4.3 Baselines

We compare our method against the following baselines. *Null-text* [46] inverts real images with corresponding captions into the text embedding of the unconditional part of the classifier-free diffusion model. *SDEdit* [44] introduces a stochastic differential equation to generate realistic images through an iterative denoising process. *Pix2pix-zero* [49] edits the real image to find the potential direction from the source to the target words. *DDIM with word swap* [49] performs DDIM sampling with an edited prompt generated by swapping the source word with the target. We use the official published codes for the baselines in our comparison to StyleDiffusion. We also ablate variants of StyleDiffusion.

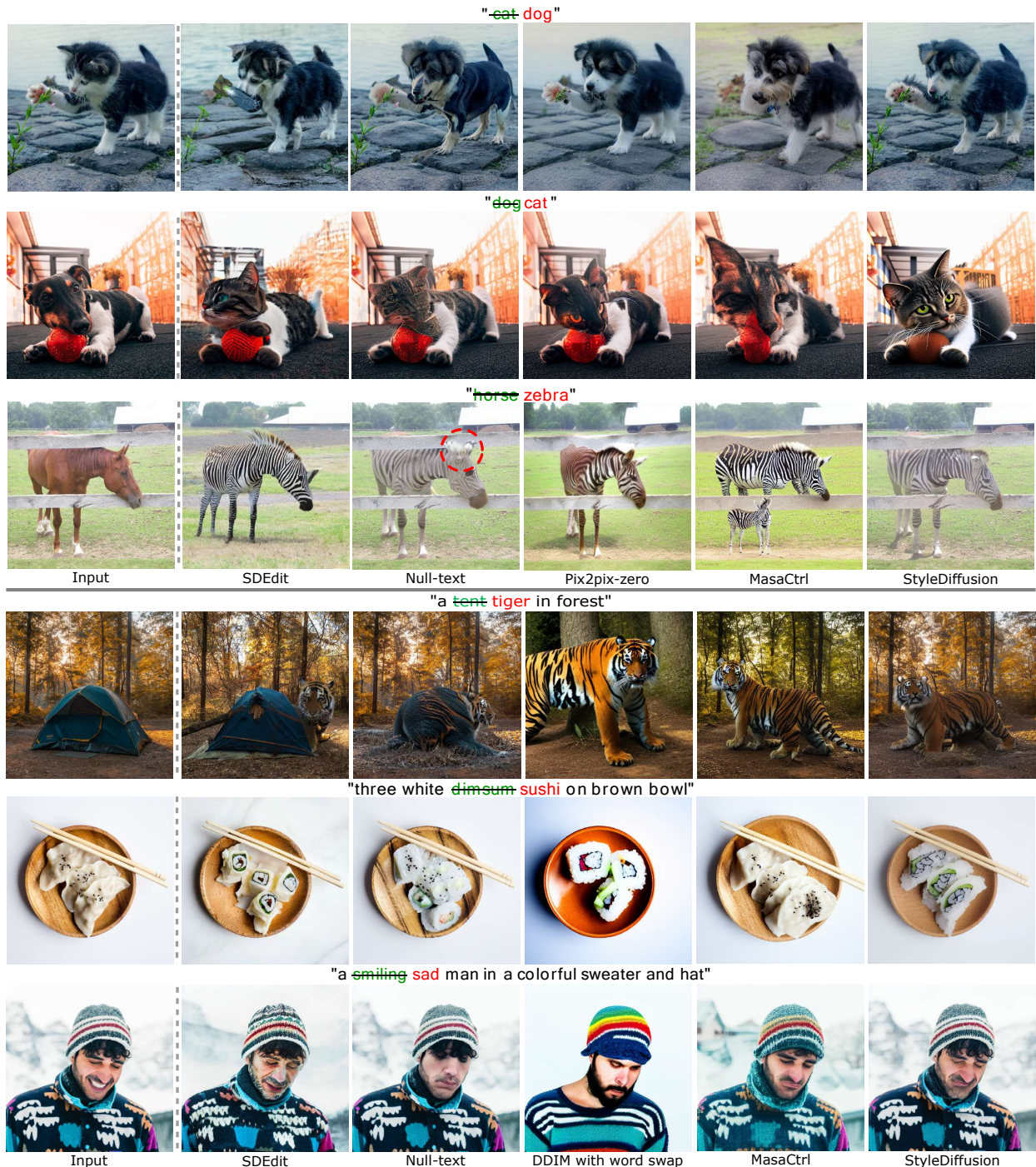


Figure 9 Comparisons with different baselines for real images. Our method achieves realistic editing of both style and structured objects, while preserving the structure of the input image (last column).

Table 2 Comparison to baselines on three metrics. *DDIM: DDIM inversion with word swap. Although *DDIM with word swap* achieves the best Clipscore, it not only changes the background, but also modifies the structure of the selected region, as can be seen in Fig. 9(last three rows, fourth column).

Metric	Structure-dist↓	NS-LPIPS↓	Clipscore↑
*DDIM	0.092	0.4131	81.9%
SDEdit	0.046	0.2473	78.0%
Null-text	0.027	0.1480	75.2%
MasaCtrl	0.039	0.2259	80.4%
Ours	0.026	0.1165	77.9%

Table 3 Inference time and PSNR/SSIM. We have better reconstruction quality with a small computational overhead.

	Inference Time↓	PSNR↑/SSIM↑
Null-text	0.28s	31.314/0.730
Ours	0.30s	31.523/0.751

5 Experiments

5.1 Qualitative and quantitative results

Fig. 9 presents a comparison between the baselines and our method. *SDEdit* [44] fails to generate high-quality images, such as dog or cat faces (second column). *Pix2pix-zero* [49] synthesizes better results, but it also modifies the non-selected region, such as removing the plant when translating cat → dog. The official implementation of *pix2pix-zero* [49] provides the editing directions (e.g, cat ↔ dog), and we directly use them. Note that *pix2pix-zero* [49] requires that the editing directions are calculated in advance, while our method does not require this. Fig. 9(last three rows, fourth column) shows that *DDIM with word swap* largely modifies both the background and the structural information of the foreground. *MasaCtrl* [10] is designed for non-rigid editing and tries to maintain content consistency after editing. It often changes the shape of objects when translating from one to another (Fig. 9(fifth column)). For example, when translating dog to cat, although *MasaCtrl* successfully performs the translation, it changes the shape, such as making the head of the cat larger than in the original image (Fig. 9(second row, the fifth column)). Our method successfully edits the target-specific object, resulting in a high-quality image, indicating that our proposed method has more accurate editing capabilities.

We evaluate the performance of the proposed method on the collected dataset. Tab. 2 reports, in terms of both Structure distance and NS-LPIPS, that the proposed method achieves the best score, indicates that we have superior capabilities to preserve structural

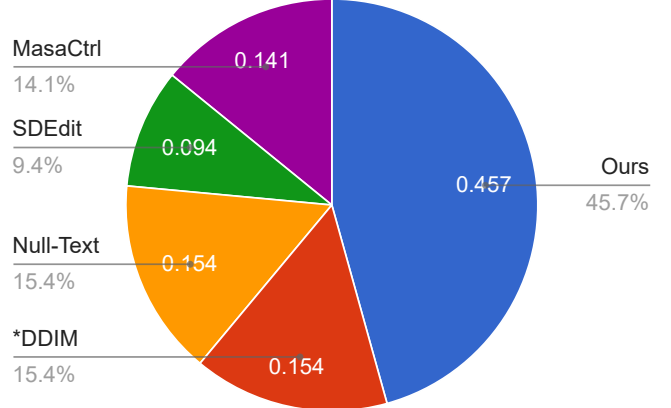


Figure 10 We conduct a forced-choice user study and ask subjects to select the results according to “*Which figure does best preserve the input image structure and matches target prompt style?*”.

information. In terms of Clipscore, we get a better score than Null-text (i.e., 77.9% vs 75.2%), and a comparative result with SDEdit. *DDIM with word swap* achieves the best Clipscore. However, *DDIM with word swap* not only changes the background, but also modifies the structure of the selected-regions (see Fig. 9(last three rows, fourth column)). Note that we do not compare to *pix2pix-zero* [49] in Fig. 9(last three rows), since it first needs to compute the textual embedding directions with thousands of sentences using GPT-3 [9]. We also evaluate the reconstruction quality and the inference time for each timestep. As reported in Tab. 3, we achieve the best PSNR/SSIM scores, with an acceptable time overhead.

Furthermore, we conduct a user study, asking subjects to select the results that best match the following statement: *which figure preserves the input image structure and matches the target prompt style* (Fig. 10). We apply quadruplet comparisons (forced choice) with 54 users (30 quadruplets/user). The study participants were volunteers from our college. The questionnaire consisted of 30 questions, each presenting the original image, as well as the results of various baselines and our method. Users were tasked with selecting an image in which the target image is more accurately edited compared to the original image. Each question in the questionnaire presents five options, including baselines (DDIM with word swap, Null-text, SDEdit, and MasaCtrl) and our method, from which users were instructed to choose one. A total of 54 users participated, resulting in a combined total of 1620 samples (30 questions × 1 option × 54 users) with 740 samples (45.68%) favoring our method. In the results of the user study, the values for DDIM with word swap,

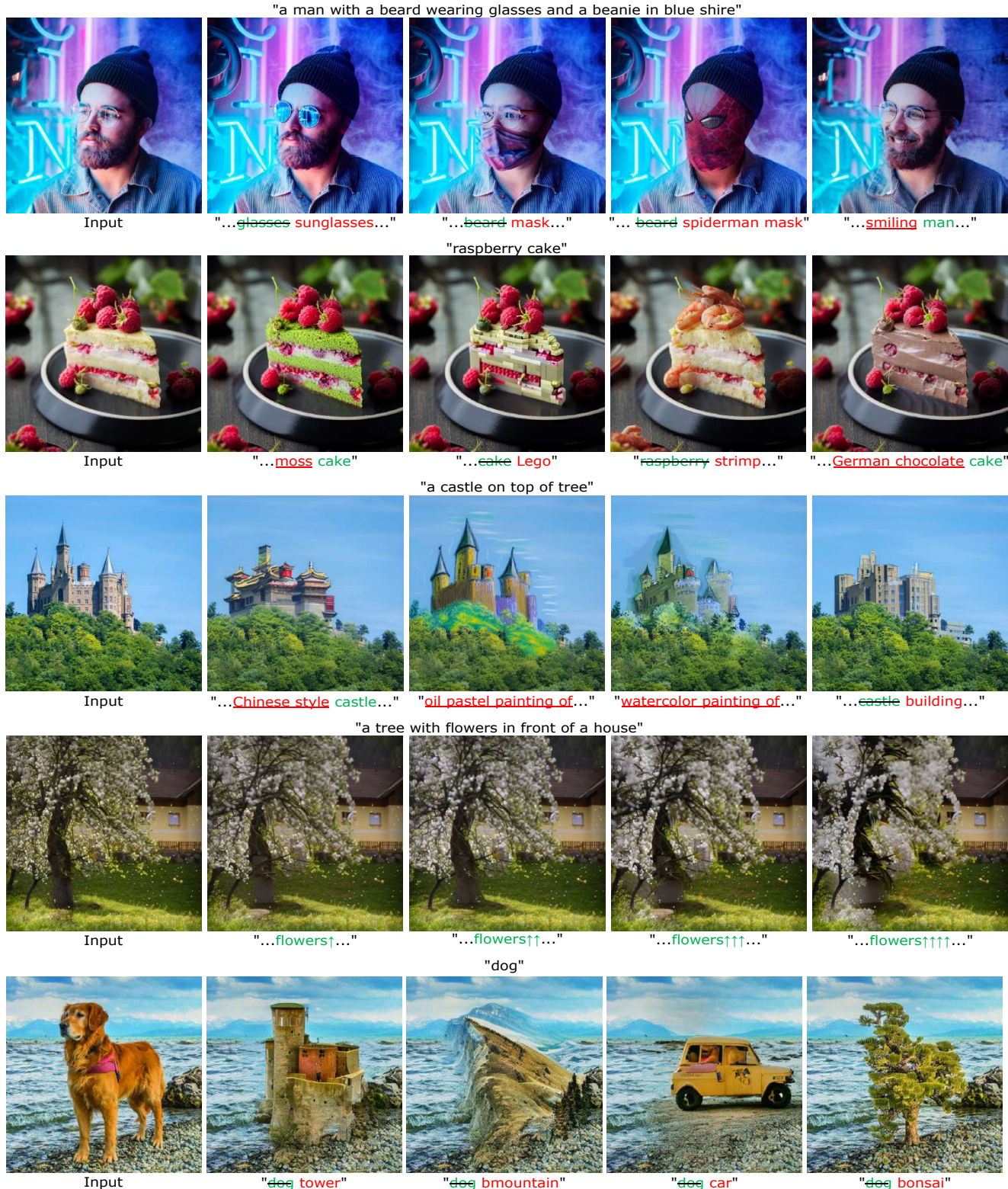


Figure 11 Examples of StyleDiffusion for editing with attention injection (replacement), refinement (adding a new phrase) or re-weighting.

NullText, SDEdit, MasaCtrl, and Ours are 15.37%, 15.43%, 9.38%, 14.14%, and 45.68%, respectively.

Fig. 11 shows that we can manipulate the inverted image with attention injection (replacement),



Figure 12 StyleDiffusion can achieve object structural changes within the range of the input image cross-attention map (e.g., “...dog” → “...sitting dog”).

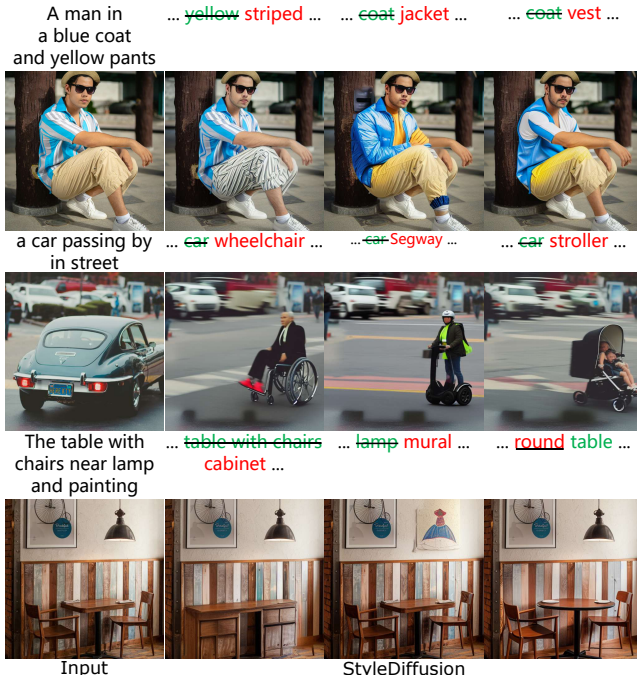


Figure 13 StyleDiffusion can be applied to many real-world applications. For example, in Fashion, rare class insertion for autonomous driving datasets, and interior design.

refinement (adding a new phrase) or re-weighting using P2Plus. For example, we translate *glasses* into *sunglasses* (Fig. 11(first row)). We add *Chinese style* (new prompts) to the source prompt (Fig. 11(third row)). We scale the attention map of the “flowers” in prompt “a tree with flowers in front of a house”, resulting in a stronger effect (Fig. 11(fourth row)). These results indicate that our approach manages to invert real images with corresponding captions into the latent space, while maintaining powerful editing capabilities.

We observe that StyleDiffusion (Fig. 12(last column)) allows for object structure modifications while preserving the identity within the range given

by the input image cross-attention map, resembling the capabilities demonstrated by Imagic [32] and MasaCtrl [10] (Fig. 12(third and fourth columns)). Furthermore, StyleDiffusion can preserve more accurate content, such as the scarf around the dog’s neck (Fig. 12(fifth column)). In contrast, Null-text [46] does not possess the capacity to accomplish such changes (Fig. 12(second column)).

StyleDiffusion can additionally be applied to many real-world applications, including object replacement in images for publicity purposes (as well as personalized advertising: see Fig. 13(first row)), dataset enrichment by adding rare objects (e.g., wheelchairs in autonomous driving datasets: Fig. 13(second row)), furniture replacement for interior design (Fig. 13(third row)), etc.

5.2 Ablation study.

Here, we evaluate the effect of each independent contribution to our method and their combinations.

5.2.1 Attention injection in the unconditional branch

Although P2P obtains satisfactory editing results with attention injection in the conditional branch, it ignores attention injection in the unconditional branch (as proposed by our P2Plus in Sec. 3.4). We experimentally observe that the self-attention maps in the unconditional branch play an important role in obtaining more accurate editing capabilities, especially when the object structure changes before and after editing of the real image are relatively large, e.g., translating *bike* to *motorcycle* in Fig. 14(left, third row). It also shows that the unconditional branch contains much useful texture and structure information, allowing us to reduce the influence of the unwanted structure of the input image.

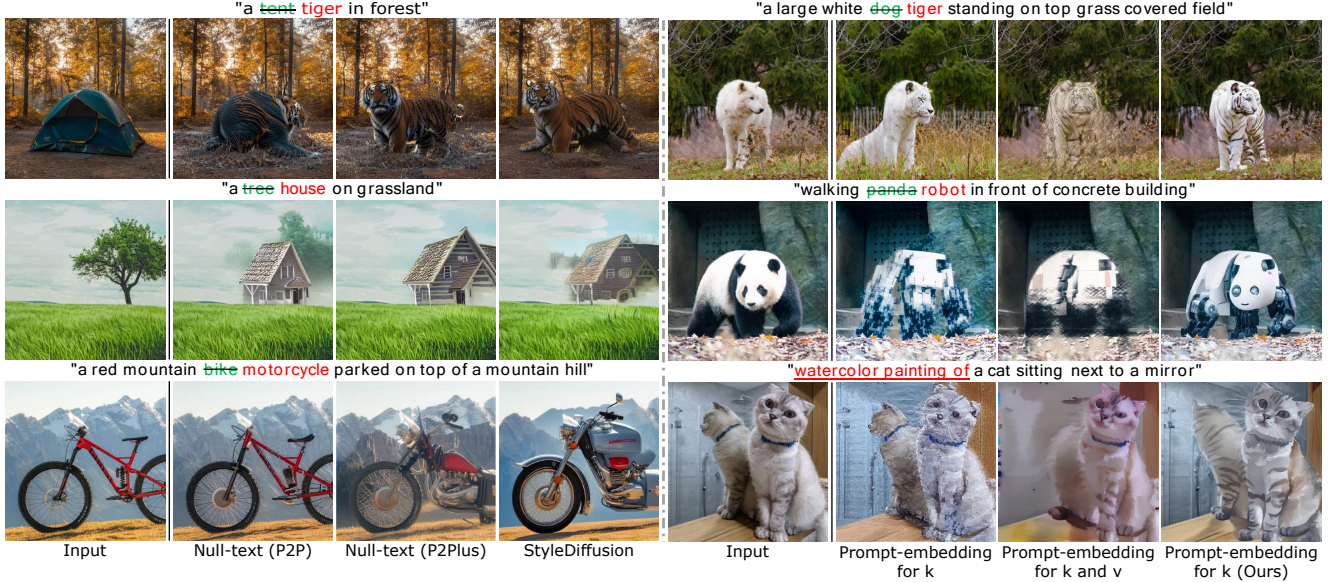


Figure 14 (Left) Additionally using the attention injection in unconditional branch improves the real image editing ability of *Null-text* (*P2P*). (Right) Comparison of variants of our method.

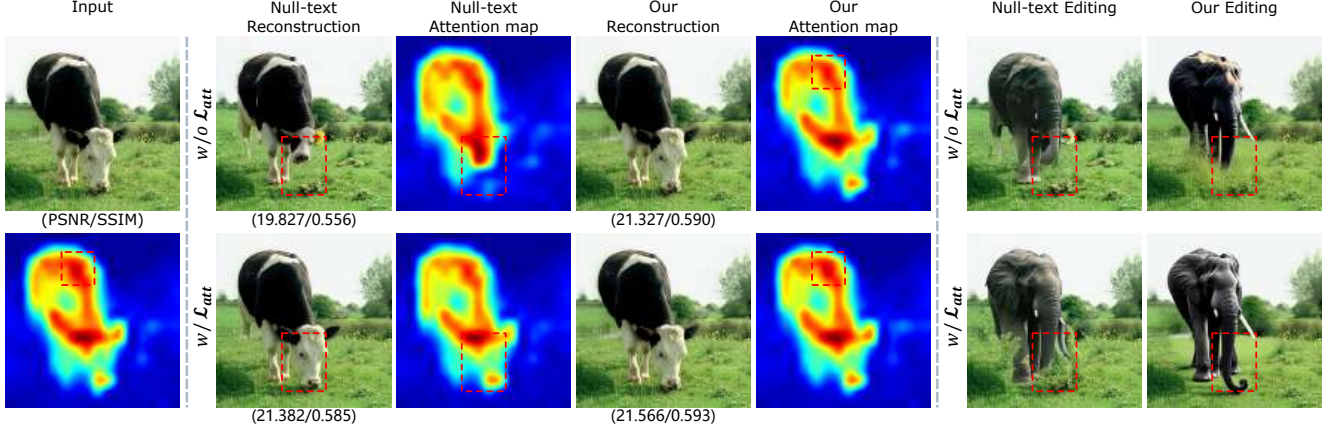


Figure 15 Reconstruction effect of attention regularization. The cross-attention map of our reconstruction image (second row, fifth column) more closely matches the one of the input image (second row, first column). Meanwhile, \mathcal{L}_{att} can improve the reconstruction quality of Null-text (second row, second column). In the last two columns, the *cow* is replaced by an *elephant* (source prompt: “cow”, target prompt: “elephant”).

5.2.2 Prompt-embedding in cross-attention layers

We evaluate variants of our method, namely (i) learning the input prompt-embedding for the *key* linear layer and freezing the input of the *value* linear layer with the one provided by the user, and (ii) learning the prompt-embedding for both *key* and *value* linear layers. As Fig. 14(right) shows, the two variants fail to edit the image according to the target prompt. Our method successfully modifies the real image with the target prompt, and produces realistic results.

5.2.3 Attention regularization

We perform an ablation study of attention regularization. Fig. 15 shows that the system fails to

reconstruct partial object information (e.g., the nose in Fig. 15(first row, second column)), and learns a less accurate attention map (e.g., the nose attention map in Fig. 15(first row, third column)). Our method not only synthesizes high-quality images, but also learns a better attention map even than the one generated by DDIM inversion (Fig. 15(second row, first column)).

5.2.4 Value-embedding optimization

Fig. 16 illustrates the reconstruction and editing results of value-embedding optimization, that is, similar to our method extracting the prompt-embedding from the input image but directly optimizing the input textual embedding. Value-embedding optimization fails to reconstruct the input image. Null-text [46]



Figure 16 Value-embedding optimization. We compare our method (right) to the one (middle) in which we directly optimize the input textual embedding for the *value* linear layer while freezing the input of the *key* linear layer. As can be seen (middle), this approach leads to an inaccurate reconstruction, resulting in the dog's face not being completely reconstructed.

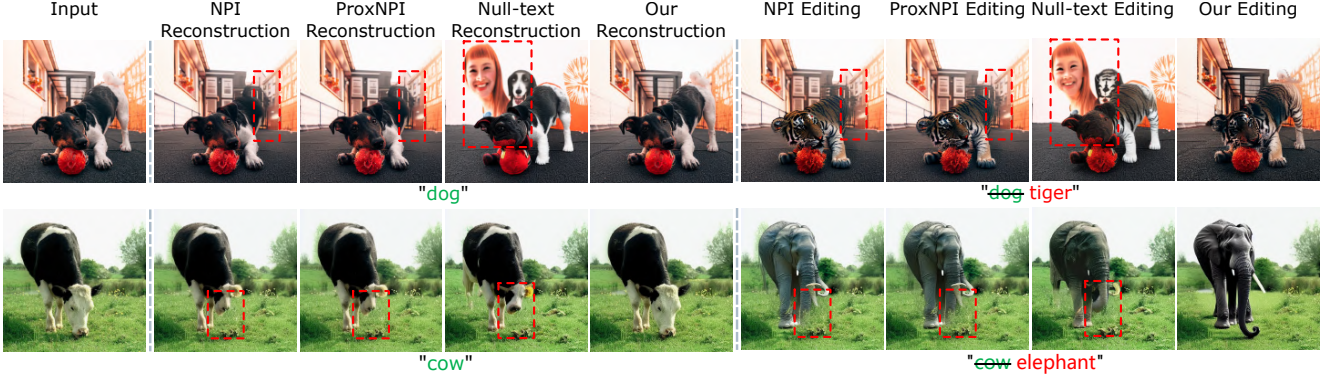


Figure 17 Both the optimization-free methods NPI and ProxNPI (second and third columns, sixth and seventh columns) show limitations in reconstructing and editing real images with complex structures and content.



Figure 18 StyleDiffusion with SDEdit. From left to right: input image, SDEdit, applying SDEdit after StyleDiffusion inversion, and applying P2Plus after StyleDiffusion inversion. It is evident that StyleDiffusion+SDEdit significantly improves the fidelity of the input image compared to SDEdit alone.

draws a similar conclusion that optimizing both the input textual embedding for the *value* and *key* linear layers results in lower editing accuracy.

5.2.5 StyleDiffusion with SDEdit

After inverting a real image with StyleDiffusion, we leverage SDEdit to edit it. Only using SDEdit, the results suffer from unwanted changes, such as the orientation of the dog (Fig. 18(first row, second

column) and the texture detail of the leg of the dog (Fig. 18(second row, second column)). While combining StyleDiffusion and SDEdit significantly enhances the fidelity to the input image (see Fig. 18(third column)). This indicates our method exhibits robust performance when combining different editing techniques (e.g., SDEdit and P2Plus).

5.2.6 Comparison with optimization-free methods

Recently, some methods have been proposed [23, 45] that do not use optimization. Negative-prompt inversion (NPI) [45] replaces the null-text embedding of the unconditional branch with the textural embedding in SD to implement reconstruction and editing. Proximal Negative-Prompt Inversion (ProxNPI) [23] attempts to enhance NPI by introducing regularization terms using proximal function and reconstruction

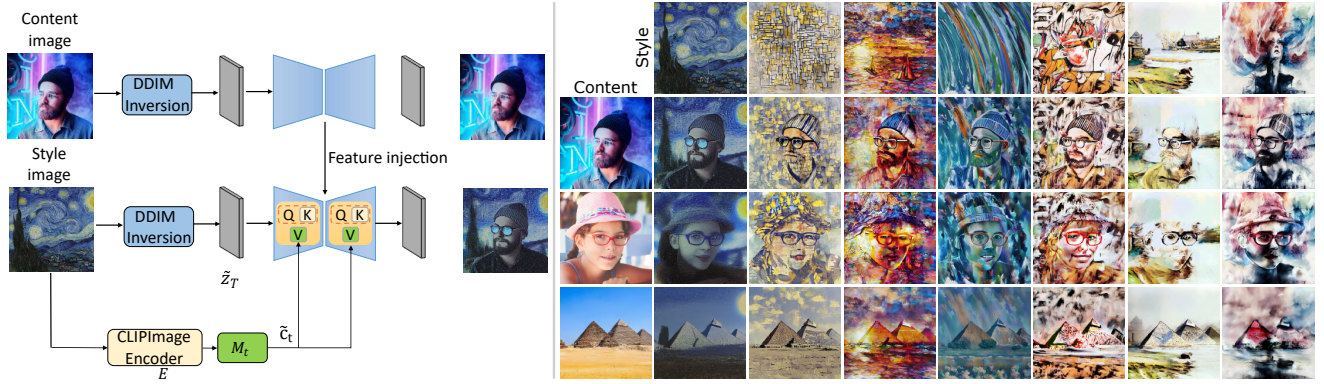


Figure 20 StyleDiffusion for style transfer. (Left) our framework for style transfer. Given a content image, we use DDIM inversion to generate a series of timestep-related latent codes. They are then progressively denoised using DDIM sampling. During this process, we extract the spatial features from the decoder layers. These spatial features are injected into the corresponding layers of StyleDiffusion model. Note we first optimize StyleDiffusion to reconstruct the style image, then use both the learned-well M_t and the extracted content feature to perform the style transfer. This approach allows us to efficiently transfer the desired artistic style to the content image without the need for additional optimization on the content image. (Right) results of style transfer with StyleDiffusion.

guidance based on the foundation of NPI. While these methods do not require optimizing parameters to achieve the inversion of real images, like to the method shown in Fig. 1, they suffer from challenges when reconstructing and editing images containing intricate content and structure (see Fig. 17(second and third columns, sixth and seventh columns)). Due to the absence of an optimization process in these methods, it is not possible to utilize attention loss to refine the attention maps like Null-text+ \mathcal{L}_{att} (Fig. 15), consequently limiting the potential for enhancing reconstruction and editing quality.

5.2.7 StyleDiffusion for style transfer

As a final illustration, we show that StyleDiffusion can be used to perform style transfer. Fig. 20(left) shows how, given a content image, we use DDIM inversion to generate a series of timestep-related latent codes. They are then progressively denoised using DDIM sampling. During this process, we extract the spatial features from the decoder layers. These spatial features are injected into the corresponding layers of StyleDiffusion model. Note that we first optimize StyleDiffusion to reconstruct the style image, then use both the well-learned M_t and the extracted content feature to perform the style transfer. Fig. 20(right) shows that we can successfully combine both content and style images, and perform style transfer.

6 Conclusions and Limitations

We propose a new method for real image editing. We invert the real image into the input of the *value* linear mapping network in the cross-attention layers,

and freeze the input of the *key* linear layer with the textual embedding provided by the user. This allows us to learn initial attention maps, and an approximate trajectory to reconstruct the real image. We introduce a new attention regularization to preserve the attention maps after editing, enabling us to obtain more accurate editing capabilities. In addition, we propose attention injection in the unconditional branch of the classifier-free diffusion model (P2Plus), further improving the editing capabilities, especially when both source and target prompts have a large domain shift.

While StyleDiffusion successfully modifies the real image, it still suffers from some limitations. Our method fails to generate satisfying images when the object in the real image has a rare pose (Fig. 19(left)), or when both the source and the target prompts have a large semantic shift (Fig. 19(right)).

Declaration of competing interest

The authors have no competing interests to declare relevant to the content in this study.

References

- [1] R. Abdal, Y. Qin, and P. Wonka. Image2stylegan: How to embed images into the stylegan latent space? In *Proceedings of the IEEE/CVF International Conference on Computer Vision*, pages 4432–4441, 2019.
- [2] R. Abdal, Y. Qin, and P. Wonka. Image2stylegan++: How to edit the embedded images? In *Proceedings of the IEEE/CVF conference on computer vision and pattern recognition*, pages 8296–8305, 2020.
- [3] Y. Alaluf, O. Tov, R. Mokady, R. Gal, and A. H.

Bermano. Hyperstyle: Stylegan inversion with hypernetworks for real image editing, 2021.

[4] M. Armandpour, H. Zheng, A. Sadeghian, A. Sadeghian, and M. Zhou. Re-imagine the negative prompt algorithm: Transform 2d diffusion into 3d, alleviate janus problem and beyond. *arXiv preprint arXiv:2304.04968*, 2023.

[5] O. Avrahami, K. Aberman, O. Fried, D. Cohen-Or, and D. Lischinski. Break-a-scene: Extracting multiple concepts from a single image. *arXiv preprint arXiv:2305.16311*, 2023.

[6] O. Avrahami, O. Fried, and D. Lischinski. Blended latent diffusion. *arXiv preprint arXiv:2206.02779*, 2022.

[7] O. Avrahami, D. Lischinski, and O. Fried. Blended diffusion for text-driven editing of natural images. In *Proceedings of the IEEE/CVF Conference on Computer Vision and Pattern Recognition*, pages 18208–18218, 2022.

[8] D. Bahdanau, K. Cho, and Y. Bengio. Neural machine translation by jointly learning to align and translate. *arXiv preprint arXiv:1409.0473*, 2014.

[9] T. Brown, B. Mann, N. Ryder, M. Subbiah, J. D. Kaplan, P. Dhariwal, A. Neelakantan, P. Shyam, G. Sastry, A. Askell, et al. Language models are few-shot learners. *Advances in neural information processing systems*, 33:1877–1901, 2020.

[10] M. Cao, X. Wang, Z. Qi, Y. Shan, X. Qie, and Y. Zheng. Masactr: Tuning-free mutual self-attention control for consistent image synthesis and editing. *arXiv preprint arXiv:2304.08465*, 2023.

[11] M. Chen, I. Laina, and A. Vedaldi. Training-free layout control with cross-attention guidance. *arXiv preprint arXiv:2304.03373*, 2023.

[12] X. Chen, H. Fang, T.-Y. Lin, R. Vedantam, S. Gupta, P. Dollár, and C. L. Zitnick. Microsoft coco captions: Data collection and evaluation server. *arXiv preprint arXiv:1504.00325*, 2015.

[13] G. Couairon, J. Verbeek, H. Schwenk, and M. Cord. Diffedit: Diffusion-based semantic image editing with mask guidance. *arXiv preprint arXiv:2210.11427*, 2022.

[14] A. Creswell and A. A. Bharath. Inverting the generator of a generative adversarial network. *IEEE transactions on neural networks and learning systems*, 30(7):1967–1974, 2018.

[15] P. Dhariwal and A. Nichol. Diffusion models beat gans on image synthesis. *Advances in Neural Information Processing Systems*, 34:8780–8794, 2021.

[16] W. Dong, S. Xue, X. Duan, and S. Han. Prompt tuning inversion for text-driven image editing using diffusion models. *arXiv preprint arXiv:2305.04441*, 2023.

[17] O. Gafni, A. Polyak, O. Ashual, S. Sheynin, D. Parikh, and Y. Taigman. Make-a-scene: Scene-based text-to-image generation with human priors. *arXiv preprint arXiv:2203.13131*, 2022.

[18] R. Gal, Y. Alaluf, Y. Atzmon, O. Patashnik, A. H. Bermano, G. Chechik, and D. Cohen-Or. An image is worth one word: Personalizing text-to-image generation using textual inversion. *arXiv preprint arXiv:2208.01618*, 2022.

[19] R. Gal, M. Arar, Y. Atzmon, A. H. Bermano, G. Chechik, and D. Cohen-Or. Encoder-based domain tuning for fast personalization of text-to-image models. *arXiv preprint arXiv:2302.12228*, 2023.

[20] R. Gal, O. Patashnik, H. Maron, G. Chechik, and D. Cohen-Or. Stylegan-nada: Clip-guided domain adaptation of image generators. *arXiv preprint arXiv:2108.00946*, 2021.

[21] L. Goetschalckx, A. Andonian, A. Oliva, and P. Isola. Ganalyze: Toward visual definitions of cognitive image properties. pages 5744–5753, 2019.

[22] I. Han, S. Yang, T. Kwon, and J. C. Ye. Highly personalized text embedding for image manipulation by stable diffusion. *arXiv preprint arXiv:2303.08767*, 2023.

[23] L. Han, S. Wen, Q. Chen, Z. Zhang, K. Song, M. Ren, R. Gao, Y. Chen, D. Liu, Q. Zhangli, et al. Improving negative-prompt inversion via proximal guidance. *arXiv preprint arXiv:2306.05414*, 2023.

[24] A. Hertz, R. Mokady, J. Tenenbaum, K. Aberman, Y. Pritch, and D. Cohen-Or. Prompt-to-prompt image editing with cross attention control. *arXiv preprint arXiv:2208.01626*, 2022.

[25] J. Hessel, A. Holtzman, M. Forbes, R. L. Bras, and Y. Choi. CLIPScore: a reference-free evaluation metric for image captioning. In *EMNLP*, 2021.

[26] J. Ho and T. Salimans. Classifier-free diffusion guidance. In *NeurIPS 2021 Workshop on Deep Generative Models and Downstream Applications*, 2021.

[27] R. Huang, M. W. Lam, J. Wang, D. Su, D. Yu, Y. Ren, and Z. Zhao. Fastdiff: A fast conditional diffusion model for high-quality speech synthesis. *arXiv preprint arXiv:2204.09934*, 2022.

[28] A. Jahanian, L. Chai, and P. Isola. On the “steerability” of generative adversarial networks. 2020.

[29] M. Jeong, H. Kim, S. J. Cheon, B. J. Choi, and N. S. Kim. Diff-tts: A denoising diffusion model for text-to-speech. *arXiv preprint arXiv:2104.01409*, 2021.

[30] X. Jia, Y. Zhao, K. C. Chan, Y. Li, H. Zhang, B. Gong, T. Hou, H. Wang, and Y.-C. Su. Taming encoder for zero fine-tuning image customization with text-to-image diffusion models. *arXiv preprint arXiv:2304.02642*, 2023.

[31] M. Kang, J.-Y. Zhu, R. Zhang, J. Park, E. Shechtman, S. Paris, and T. Park. Scaling up gans for text-to-image synthesis. 2023.

[32] B. Kawar, S. Zada, O. Lang, O. Tov, H.-T. Chang, T. Dekel, I. Mosseri, and M. Irani. Imagic: Text-based real image editing with diffusion models. *ArXiv*, abs/2210.09276, 2022.

[33] L. Khachatryan, A. Movsisyan, V. Tadevosyan, R. Henschel, Z. Wang, S. Navasardyan, and H. Shi. Text2video-zero: Text-to-image diffusion models are zero-shot video generators. *arXiv preprint arXiv:2303.13439*, 2023.

[34] G. Kim, T. Kwon, and J. C. Ye. Diffusionclip: Text-guided diffusion models for robust image manipulation. In *Proceedings of the IEEE/CVF Conference on Computer Vision and Pattern Recognition*, pages 2426–2435, 2022.

[35] D. Kingma and J. Ba. Adam: A method for stochastic optimization. 2014.

[36] Y. Koizumi, H. Zen, K. Yatabe, N. Chen, and M. Bacchiani. Specgrad: Diffusion probabilistic model based neural vocoder with adaptive noise spectral shaping. *arXiv preprint arXiv:2203.16749*, 2022.

[37] N. Kumari, B. Zhang, R. Zhang, E. Shechtman, and J.-Y. Zhu. Multi-concept customization of text-to-image diffusion. *arXiv preprint arXiv:2212.04488*, 2022.

[38] N. Kumari, B. Zhang, R. Zhang, E. Shechtman, and J.-Y. Zhu. Multi-concept customization of text-to-image diffusion. In *Proceedings of the IEEE/CVF Conference on Computer Vision and Pattern Recognition*, pages 1931–1941, 2023.

[39] M. Kwon, J. Jeong, and Y. Uh. Diffusion models already have a semantic latent space. *arXiv preprint arXiv:2210.10960*, 2022.

[40] E. Levin and O. Fried. Differential diffusion: Giving each pixel its strength. *arXiv preprint arXiv:2306.00950*, 2023.

[41] C.-H. Lin, J. Gao, L. Tang, T. Takikawa, X. Zeng, X. Huang, K. Kreis, S. Fidler, M.-Y. Liu, and T.-Y. Lin. Magic3d: High-resolution text-to-3d content creation. In *Proceedings of the IEEE/CVF Conference on Computer Vision and Pattern Recognition*, pages 300–309, 2023.

[42] Z. C. Lipton and S. Tripathi. Precise recovery of latent vectors from generative adversarial networks. *arXiv preprint arXiv:1702.04782*, 2017.

[43] G. Liu, H. Sun, J. Li, F. Yin, and Y. Yang. Accelerating diffusion models for inverse problems through shortcut sampling. *arXiv preprint arXiv:2305.16965*, 2023.

[44] C. Meng, Y. Song, J. Song, J. Wu, J.-Y. Zhu, and S. Ermon. Sdedit: Image synthesis and editing with stochastic differential equations. *arXiv preprint arXiv:2108.01073*, 2021.

[45] D. Miyake, A. Iohara, Y. Saito, and T. Tanaka. Negative-prompt inversion: Fast image inversion for editing with text-guided diffusion models. *arXiv preprint arXiv:2305.16807*, 2023.

[46] R. Mokady, A. Hertz, K. Aberman, Y. Pritch, and D. Cohen-Or. Null-text inversion for editing real images using guided diffusion models. *arXiv preprint arXiv:2211.09794*, 2022.

[47] C. Mou, X. Wang, J. Song, Y. Shan, and J. Zhang. Dragondiffusion: Enabling drag-style manipulation on diffusion models. *arXiv preprint arXiv:2307.02421*, 2023.

[48] A. Nichol, P. Dhariwal, A. Ramesh, P. Shyam, P. Mishkin, B. McGrew, I. Sutskever, and M. Chen. Glide: Towards photorealistic image generation and editing with text-guided diffusion models. *arXiv preprint arXiv:2112.10741*, 2021.

[49] G. Parmar, K. K. Singh, R. Zhang, Y. Li, J. Lu, and J.-Y. Zhu. Zero-shot image-to-image translation. *arXiv preprint arXiv:2302.03027*, 2023.

[50] O. Patashnik, Z. Wu, E. Shechtman, D. Cohen-Or, and D. Lischinski. Styleclip: Text-driven manipulation of stylegan imagery. *arXiv preprint arXiv:2103.17249*, 2021.

[51] B. Poole, A. Jain, J. T. Barron, and B. Mildenhall. Dreamfusion: Text-to-3d using 2d diffusion. *arXiv preprint arXiv:2209.14988*, 2022.

[52] Z. Qiu, W. Liu, H. Feng, Y. Xue, Y. Feng, Z. Liu, D. Zhang, A. Weller, and B. Schölkopf. Controlling text-to-image diffusion by orthogonal finetuning. *arXiv preprint arXiv:2306.07280*, 2023.

[53] A. Ramesh, P. Dhariwal, A. Nichol, C. Chu, and M. Chen. Hierarchical text-conditional image generation with clip latents. *arXiv preprint arXiv:2204.06125*, 2022.

[54] E. Richardson, Y. Alaluf, O. Patashnik, Y. Nitzan, Y. Azar, S. Shapiro, and D. Cohen-Or. Encoding in style: a stylegan encoder for image-to-image translation. *arXiv preprint arXiv:2008.00951*, 2020.

[55] D. Roich, R. Mokady, A. H. Bermano, and D. Cohen-Or. Pivotal tuning for latent-based editing of real images. *ACM Transactions on Graphics (TOG)*, 2022.

[56] R. Rombach, A. Blattmann, D. Lorenz, P. Esser, and B. Ommer. High-resolution image synthesis with latent diffusion models, 2021.

[57] N. Ruiz, Y. Li, V. Jampani, Y. Pritch, M. Rubinstein, and K. Aberman. Dreambooth: Fine tuning text-to-image diffusion models for subject-driven generation. *arXiv preprint arXiv:2208.12242*, 2022.

[58] C. Saharia, W. Chan, S. Saxena, L. Li, J. Whang, E. Denton, S. K. S. Ghasemipour, B. K. Ayan, S. S. Mahdavi, R. G. Lopes, T. Salimans, T. Salimans, J. Ho, D. J. Fleet, and M. Norouzi. Photorealistic text-to-image diffusion models with deep language understanding. *arXiv preprint arXiv:2205.11487*, 2022.

[59] A. Sauer, T. Karras, S. Laine, A. Geiger, and T. Aila. StyleGAN-T: Unlocking the power of GANs for fast large-scale text-to-image synthesis. In *International Conference on Machine Learning*, volume abs/2301.09515, 2023.

[60] J. Song, C. Meng, and S. Ermon. Denoising diffusion implicit models. In *International Conference on Learning Representations*, 2020.

[61] Y. Tewel, R. Gal, G. Chechik, and Y. Atzmon. Key-locked rank one editing for text-to-image personalization. *arXiv preprint arXiv:2305.01644*, 2023.

[62] O. Tov, Y. Alaluf, Y. Nitzan, O. Patashnik, and D. Cohen-Or. Designing an encoder for stylegan image manipulation. *arXiv preprint arXiv:2102.02766*, 2021.

[63] N. Tumanyan, O. Bar-Tal, S. Bagon, and T. Dekel. Splicing vit features for semantic appearance transfer. In *Proceedings of the IEEE/CVF Conference on Computer Vision and Pattern Recognition*, pages 10748–10757, 2022.

[64] N. Tumanyan, M. Geyer, S. Bagon, and T. Dekel. Plug-and-play diffusion features for text-driven image-to-image translation. In *Proceedings of the IEEE/CVF Conference on Computer Vision and Pattern Recognition (CVPR)*, pages 1921–1930, June 2023.

[65] D. Valevski, M. Kalman, Y. Matias, and Y. Leviathan. Unitune: Text-driven image editing by fine tuning an image generation model on a single image. *arXiv preprint arXiv:2210.09477*, 2022.

[66] A. Vaswani, N. Shazeer, N. Parmar, J. Uszkoreit, L. Jones, A. N. Gomez, L. Kaiser, and I. Polosukhin. Attention is all you need. In *Advances in Neural Information Processing Systems*, volume 30, 2017.

[67] Z. Wang, C. Lu, Y. Wang, F. Bao, C. Li, H. Su, and J. Zhu. Prolificdreamer: High-fidelity and diverse text-to-3d generation with variational score distillation. *arXiv preprint arXiv:2305.16213*, 2023.

[68] C. Wu, L. Herranz, X. Liu, J. Van De Weijer, B. Raducanu, et al. Memory replay gans: Learning to generate new categories without forgetting. *Advances in Neural Information Processing Systems*, 31, 2018.

[69] J. Z. Wu, Y. Ge, X. Wang, W. Lei, Y. Gu, W. Hsu, Y. Shan, X. Qie, and M. Z. Shou. Tune-a-video: One-shot tuning of image diffusion models for text-to-video generation. *arXiv preprint arXiv:2212.11565*, 2022.

[70] W. Xia, Y. Zhang, Y. Yang, J.-H. Xue, B. Zhou, and M.-H. Yang. Gan inversion: A survey, 2021.

[71] G. Xiao, T. Yin, W. T. Freeman, F. Durand, and S. Han. Fastcomposer: Tuning-free multi-subject image generation with localized attention. *arXiv preprint arXiv:2305.10431*, 2023.

[72] E. Xie, L. Yao, H. Shi, Z. Liu, D. Zhou, Z. Liu, J. Li, and Z. Li. Diffit: Unlocking transferability of large diffusion models via simple parameter-efficient fine-tuning. *arXiv preprint arXiv:2304.06648*, 2023.

[73] R. A. Yeh, C. Chen, T. Y. Lim, A. G. Schwing, M. Hasegawa-Johnson, and M. N. Do. Semantic image inpainting with deep generative models, 2017.

[74] J. Yu, Y. Xu, J. Y. Koh, T. Luong, G. Baid, Z. Wang, V. Vasudevan, A. Ku, Y. Yang, B. K. Ayan, et al. Scaling autoregressive models for content-rich text-to-image generation. *arXiv preprint arXiv:2206.10789*, 2022.

[75] L. Zhang and M. Agrawala. Adding conditional control to text-to-image diffusion models, 2023.

[76] R. Zhang, P. Isola, A. A. Efros, E. Shechtman, and O. Wang. The unreasonable effectiveness of deep features as a perceptual metric. In *Proceedings of the IEEE conference on computer vision and pattern recognition*, pages 586–595, 2018.

[77] Y. Zhang, W. Dong, F. Tang, N. Huang, H. Huang, C. Ma, T.-Y. Lee, O. Deussen, and C. Xu. Prospect: Expanded conditioning for the personalization of attribute-aware image generation. *arXiv preprint arXiv:2305.16225*, 2023.

[78] Z. Zhang, Z. Huang, and J. Liao. Continuous layout editing of single images with diffusion models. *arXiv preprint arXiv:2306.13078*, 2023.

[79] D. Zhou, W. Wang, H. Yan, W. Lv, Y. Zhu, and J. Feng. Magicvideo: Efficient video generation with latent diffusion models. *arXiv preprint arXiv:2211.11018*, 2022.

[80] J. Zhu, Y. Shen, D. Zhao, and B. Zhou. In-domain gan inversion for real image editing. *arXiv preprint arXiv:2004.00049*, 2020.